ARTICLE

Identification and characterization of a small molecule AMPK activator that treats key components of type 2 diabetes and the metabolic syndrome

Barbara Cool,[1,7,*] Bradley Zinker,[5,7] William Chiou,[1] Lemma Kifle,[1] Ning Cao,[1] Matthew Perham,[1] Robert Dickinson,[1] Andrew Adler,[1] Gerard Gagne,[2] Rajesh Iyengar,[1] Gang Zhao,[1] Kennan Marsh,[3] Philip Kym,[1] Paul Jung,[4] Heidi S. Camp,[1] and Ernst Frevert[6,*]

[1] Department of Metabolic Disease Research
[2] Exploratory and Investigative Technologies
[3] Experimental Sciences
[4] Gene Expression Analysis, Abbott Laboratories, 100 Abbott Park Road, Abbott Park, Illinois 60064
[5] Present address: Metabolic Diseases, Diabetes, Pharmaceutical Research Institute, Bristol-Myers Squibb Company, P.O. Box 5400, Princeton, New Jersey 08543
[6] Present address: Exploratory Clinical Development, Novartis Pharmaceuticals Corporation, One Health Plaza, East Hanover, New Jersey 07936
[7] These authors contributed equally to this work.
*Correspondence: barbara.l.cool@abbott.com (B.C.); uli.frevert@novartis.com (E.F.)

Summary

AMP-activated protein kinase (AMPK) is a key sensor and regulator of intracellular and whole-body energy metabolism. We have identified a thienopyridone family of AMPK activators. A-769662 directly stimulated partially purified rat liver AMPK (EC_{50} = 0.8 μM) and inhibited fatty acid synthesis in primary rat hepatocytes (IC_{50} = 3.2 μM). Short-term treatment of normal Sprague Dawley rats with A-769662 decreased liver malonyl CoA levels and the respiratory exchange ratio, VCO_2/VO_2, indicating an increased rate of whole-body fatty acid oxidation. Treatment of *ob/ob* mice with 30 mg/kg b.i.d. A-769662 decreased hepatic expression of PEPCK, G6Pase, and FAS, lowered plasma glucose by 40%, reduced body weight gain and significantly decreased both plasma and liver triglyceride levels. These results demonstrate that small molecule-mediated activation of AMPK in vivo is feasible and represents a promising approach for the treatment of type 2 diabetes and the metabolic syndrome.

Introduction

Obesity and associated diseases like type 2 diabetes, the metabolic syndrome, hypertension, and atherogenic dyslipidemia are major and growing health risks. Each of these conditions is frequently associated with reduced insulin action and impaired glucose and lipid metabolism, resulting in significantly increased cardiovascular risk. AMPK, a heterotrimeric serine/threonine kinase widely recognized as a key regulator of fatty acid and glucose homeostasis (Hardie et al., 2003; Kahn et al., 2005), is emerging as an attractive target for the treatment of these conditions.

AMPK is involved in the regulation of whole-body energy metabolism, as evidenced by the fact that two adipose tissue-derived hormones, leptin and adiponectin, modulate AMPK activity (Minokoshi and Kahn, 2003; Minokoshi et al., 2002; Steinberg et al., 2003; Tomas et al., 2002; Wu et al., 2003; Yamauchi et al., 2002). AMPK appears to mediate the action of leptin in skeletal muscle where leptin-induced AMPK activation increases fatty acid oxidation. Adiponectin, previously identified as a regulator of glucose and lipid metabolism (Goldstein and Scalia, 2004), also stimulates AMPK activity in skeletal muscle and liver resulting in increased fat oxidation in muscle and liver, increased glucose transport in muscle, and decreased hepatic glucose production. The role of AMPK in regulating whole-body energy metabolism is further emphasized by studies of AMPK catalytic α2 subunit specific knockout (KO) or overexpressing mice. The α2-specific knockout mice exhibit glucose intolerance and insulin resistance, reduced muscle glycogen synthesis, and chronically elevated free fatty acid levels (Viollet et al., 2003). In a more recent study, on a high-fat diet, α2 KO animals exhibited increased body weight coupled with increased fat mass due to enlarged adipocyte cell size (Villena et al., 2004). In contrast, acute hepatic overexpression of a constitutively active α2 subunit results in reduced blood glucose and increased hepatic fatty acid oxidation, suggesting a preference for fatty acid utilization in supplying energy needs (Foretz et al., 2005).

On a cellular level, AMPK plays a role as an energy sensor and regulator. Under conditions of energy depletion, AMPK inhibits ATP-consuming pathways (e.g., fatty acid synthesis, cholesterol synthesis, and gluconeogenesis) and stimulates ATP-generating processes (e.g., fatty acid oxidation and glycolysis), thus restoring overall cellular energy homeostasis (Carling, 2004; Hardie, 2003). In regulating glucose metabolism, AMPK activation suppresses expression of two key gluconeogenic enzymes, PEPCK and glucose-6-phosphatase which in turn inhibits gluconeogenesis. This suppression of gluconeogenic gene expression has been demonstrated with the nonspecific AMPK activator, 5-aminoimidazole-4-carboxamide riboside (AICAR), in hepatoma cells (Lochhead et al., 2000) and also in vivo following adiponectin administration (Yamauchi et al., 2002) or adenovirus-mediated delivery of a constitutively active AMPK (Foretz

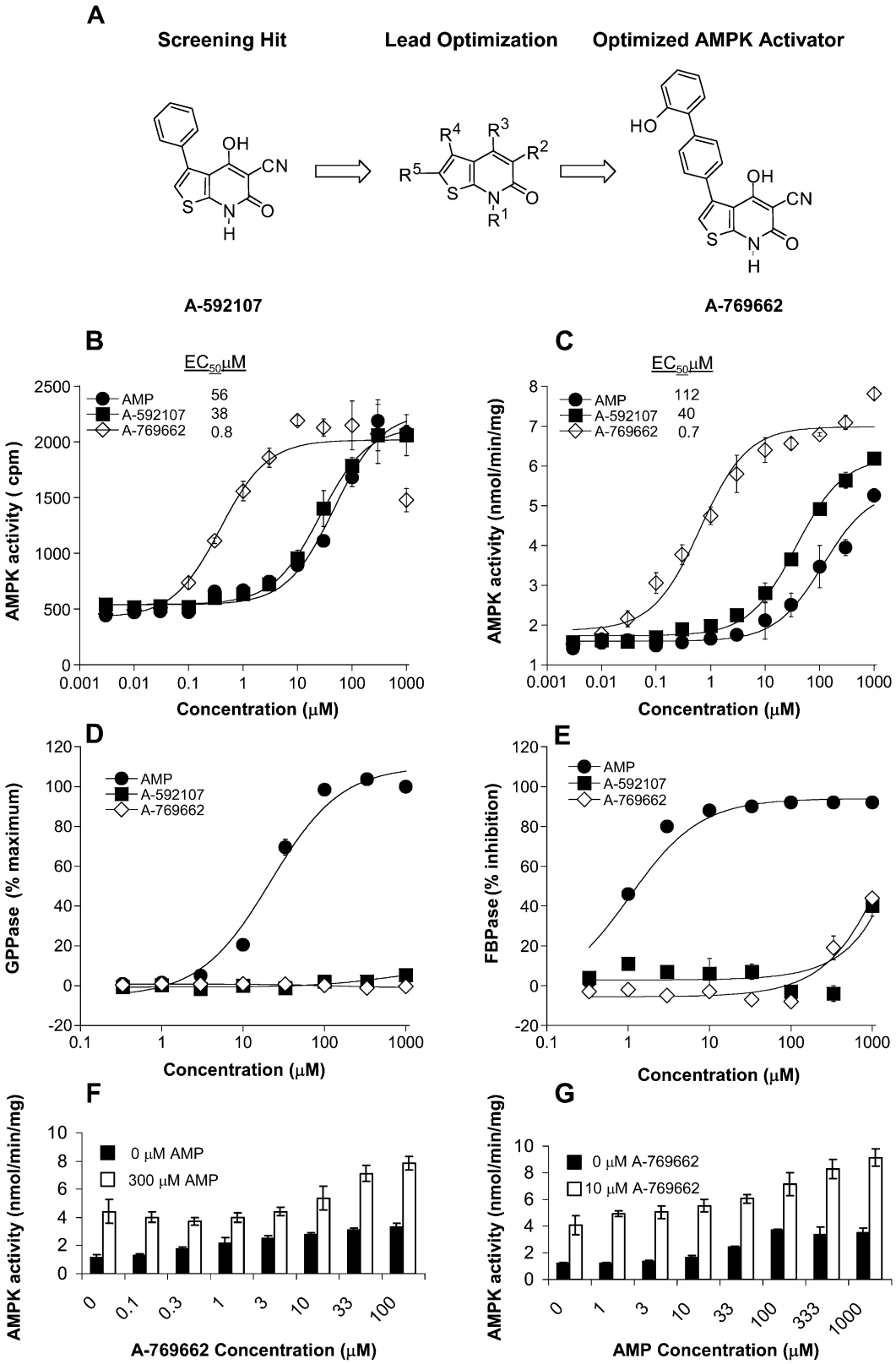

Figure 1. Thienopyridone structure, enzymatic potency, reversibility, and selectivity

A) The general structure of the thienopyridones and the structures of A-592107, the original screening hit, and A-769662, an optimized thienopyridone.
B) Stimulation of partially purified rat liver AMPK. Activity was monitored by measuring ^{33}P-phosphorylation of the SAMS peptide substrate.
C) Activation of the baculovirus/Sf9 expressed isoform of AMPK, $\alpha 1\beta 1\gamma 1$.
D) GPPase activity was measured in the presence of glycogen using a phosphoglucomutase and glucose-6 phosphate dehydrogenase-coupled spectrophotometric method. Effects of test compounds are expressed as a percent of the maximum stimulation achieved by AMP.

et al., 2005; Viana et al., 2006). In addition, AMPK activation acutely increases glucose uptake (via Glut1 and Glut4) and chronically increases Glut 4 expression (Hardie and Hawley, 2001). In lipid metabolism, AMPK activation results in the phosphorylation and inactivation of acetyl-CoA carboxylase (ACC) (Carling et al., 1987), a direct AMPK substrate, leading to decreased conversion of acetyl-CoA to malonyl CoA. AMPK activation also results in phosphorylation and activation of malonyl-CoA decarboxylase (MCD) (Saha et al., 2000), resulting in further lowering of malonyl CoA levels. Malonyl CoA allosterically inhibits carnitine palmitoyl-CoA transferase (CPT1), the enzyme responsible for transport of long chain acyl-CoAs into mitochondria for oxidation (McGarry and Brown, 1997). Therefore, a reduction in malonyl CoA levels leads to deinhibition of CPT1 and hence increases fatty acid oxidation. Additionally, as malonyl CoA is required for de novo synthesis of fatty acids, decreased malonyl CoA leads to a reduction in hepatic fatty acid synthesis (Ruderman and Prentki, 2004).

The enzymatic activity of AMPK is stimulated through phosphorylation of threonine-172 on the catalytic α subunits by an upstream AMPK kinase and through allosteric activation by AMP (Hardie et al., 2003; Hawley et al., 2003; Kemp et al., 1999) through CBS (cystathionine β-synthase) domains on the γ subunits (Scott et al., 2004). Aside from AMP and related nucleotides such as ZMP, presumed to bind at the AMP binding sites, to date, direct AMPK activators have not been described. Although the antidiabetic agents metformin and thiazolidinediones (TZDs) can stimulate AMPK activity in certain cellular environments (Fryer et al., 2002; Musi et al., 2002; Saha et al., 2004; Zang et al., 2004; Zhou et al., 2001; Zou et al., 2004), these effects appear to be indirect. AICAR, due to its intracellular conversion to ZMP, has been widely used to stimulate AMPK. However, ZMP also acts as a potent AMP analog to stimulate glycogen phosphorylase (GPPase) (Longnus et al., 2003; Young et al., 1996) and inhibit fructose-1,6-bisphosphatase (FBPase) (Vincent et al., 1991). Therefore, it is unclear whether the various metabolic effects seen with AICAR administration are mediated primarily through AMPK stimulation.

Through its central role in the regulation of glucose and lipid metabolism, AMPK is a promising molecular target for the treatment of diabetes and the metabolic syndrome (Winder and Hardie, 1999). In order to further elucidate the physiological consequences of AMPK activation we have identified and characterized a family of small molecules that directly activate AMPK in vitro and in vivo.

Results and discussion

Structure and enzymatic activity of small molecule AMPK activators

By monitoring phosphorylation of the SAMS peptide, a widely used substrate for AMPK (Davies et al., 1989), we screened a chemical library of over 700,000 compounds (Anderson et al., 2004), using partially purified rat liver AMPK and identified a nonnucleoside thienopyridone as a direct activator of AMPK (Figure 1A). The thienopyridone family is defined as shown in Figure 1A. A-592107 stimulated partially purified rat liver AMPK with a potency comparable to AMP (EC_{50} = 38 μM versus 56 μM, respectively, Figure 1B) and with similar maximal activity. Subsequent optimization of this original screening hit led to the synthesis of structurally related AMPK-activators, culminating in the identification of A-769662 (EC_{50} = 0.8 μM, Figures 1A and 1B). A-769662 was equally potent in activating the baculovirus expressed α1,β1,γ1 recombinant isoform of AMPK (EC50 = 0.7 μM, Figure 1C). To determine if A-769662 is a reversible activator, liver AMPK was preincubated with a 20-fold excess of A-769662, followed by dilution to achieve the 1× drug concentration routinely used in the standard assay format. Activation observed with or without preincubation was equivalent, indicating that A-769662-induced AMPK activation occurs by reversible binding (data not shown). Both A-592107 and A-769662 activate AMPK purified from multiple tissues and species in a dose-responsive manner with modest variations in observed EC_{50}s (Table S1 in the Supplemental Data available with this article online). EC_{50}s determined for A-769662 using partially purified AMPK extracts from rat heart, rat muscle, or human embryonic kidney cells (HEKs) were 2.2 μM, 1.9 μM, or 1.1 μM, respectively.

The enzymes GPPase and FBPase are allosterically modulated by AMP and ZMP (Longnus et al., 2003; Vincent et al., 1991; Young et al., 1996). AMP activates GPPase, whereas it inhibits FBPase. To assess the specificity of A-592107 and A-769662 for AMPK-activation, we determined their effects on these two enzymes in vitro. A-592107 and A-769662 had no effect on GPPase activity at concentrations up to 1 mM, while the EC_{50} of AMP for the activation of GPPase was 19.2 μM (Figure 1D). Similarly, neither compound showed significant inhibitory effect on FBPase at concentrations up to 100 μM, while AMP significantly inhibited FBPase (IC_{50} = 1.0 μM, Figure 1E). These results indicate that unlike AICAR/ZMP, A-592107 and A-769662 are not general AMP mimetics but selectively activate AMPK. To further establish the specificity of A-769662, we evaluated binding activity of A-769662 against a panel of 67 receptors and ion channels (Cerep, Paris, France) and found no significant cross-reactivity at a concentration of 10 μM.

The observation that A-769662 does not affect GPPase and FBPase activities (whereas AMP potently regulates these enzymes) strongly suggests that A-769662 stimulates AMPK activity in a manner that differs from AMP. To further address this issue, we evaluated the additivity of AMP and A-769662 mediated AMPK stimulation. A-769662 increased AMPK activity in the presence of a saturating concentration of AMP (Figure 1F) and AMP stimulated AMPK in the presence of a maximally efficacious concentration of A-769662 (Figure 1G). This further supports the hypothesis that A-769662 binds at a unique site that differs from that of AMP binding.

Thienopyridone efficacy in primary rat hepatocytes

Activation of AMPK increases phosphorylation of various downstream target proteins including ACC (Carling et al., 1987), a key

E) FBPase activity was determined using the substrate D-fructose-1,6-bisphosphate and colorimetric detection of free phosphate. Results are expressed as percent inhibition relative to vehicle control.

F) A-769662 dose-responsive AMPK activation and additive activation in the presence of 300 μM AMP.

G) AMP dose-responsive AMPK activation and additive activation in the presence of 10 μM A-769662.

Assay results presented in panels (**B**) through (**G**) are means ± SD from experiments run in triplicate and are representative of a minimum of two independent experiments.

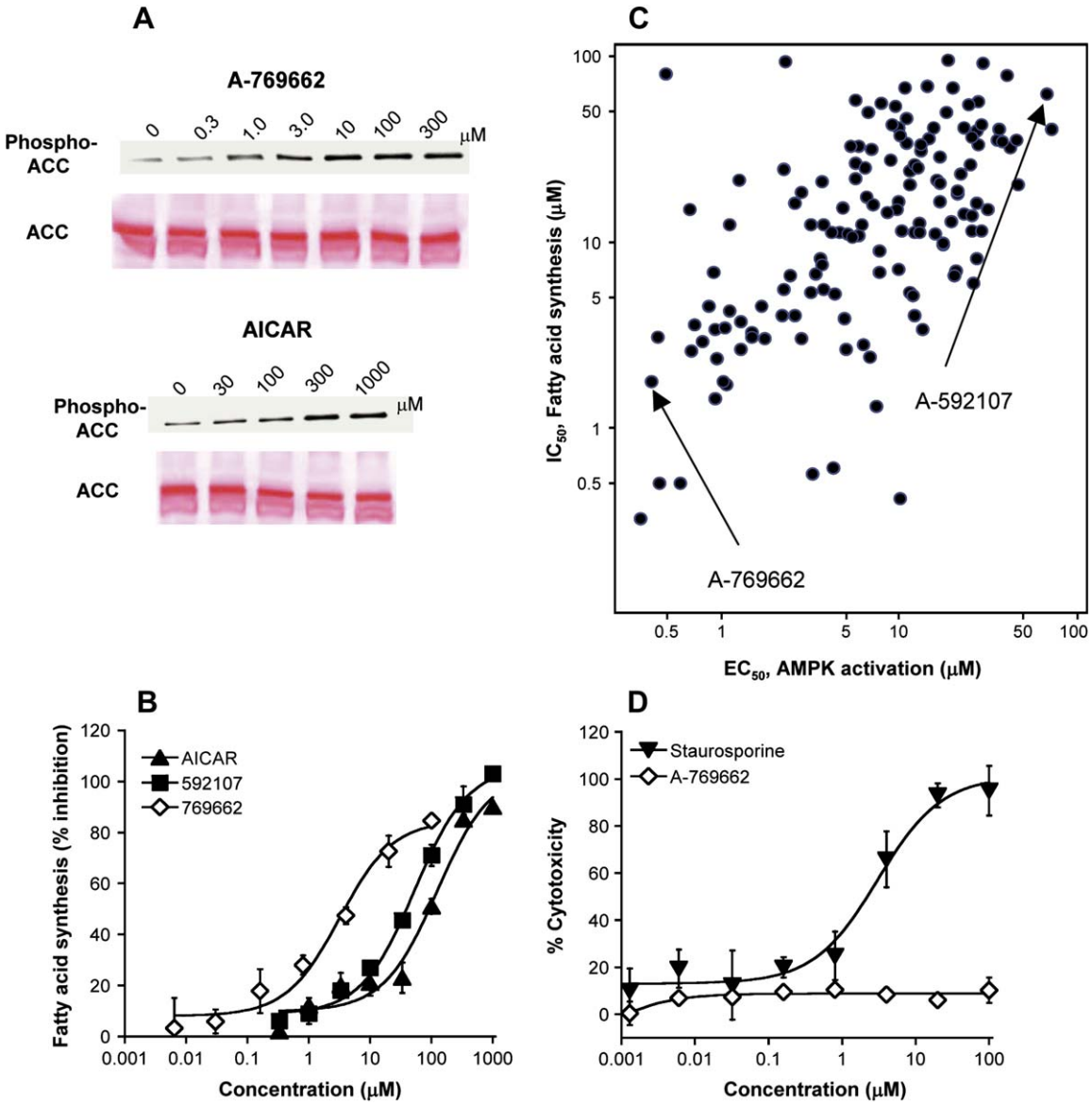

Figure 2. Thienopyridones increase ACC phosphorylation and decrease fatty acid synthesis in the absence of cytotoxicity in primary rat hepatocytes

A) Western blot analysis of total ACC or the phosphorylated form of ACC in cell lysates from primary rat hepatocytes treated for 4 hr with AICAR or A-769662.

B) Fatty acid synthesis was measured as incorporation of ^{14}C-acetate into fatty acids in primary rat hepatocytes during a 4 hr treatment with increasing concentrations of AICAR, A-592107, or A-769662. Results are given as percent inhibition of fatty acid synthesis relative to the vehicle control and are means ± SD from experiments run in triplicate and are representative of a minimum of four independent experiments.

C) Spotfire analysis showing correlation between thienopyridone potencies for AMPK activation and for inhibition of fatty acid synthesis.

D) Results of cytotoxity assays run in primary rat hepatocytes using MTS reagents and comparing a known cytotoxin, staurosporine, and A-769662. Data is from a minimum of 10 experiments run in triplicate and is given as means ± SD.

enzyme in the regulation of fatty acid metabolism. The phosphorylation and hence inactivation of ACC results in decreased levels of malonyl CoA which in turn activates CPT1 to increase fatty acid oxidation and reduce de novo fatty acid synthesis (Ruderman et al., 2003). A 4 hr treatment of primary rat hepatocytes with A-769662 or AICAR dose-dependently increased ACC phosphorylation, as detected by Western blot analysis using a phospho-specific antibody targeted to serine-79 (Figure 2A), a site specifically phosphorylated by AMPK (Davies et al., 1990). There was no commensurate change in overall ACC protein levels following drug treatment (Figure 2A). The increased ACC phosphorylation correlated with inhibition of fatty acid synthesis as measured by incorporation of ^{14}C-acetate into fatty acids, with IC_{50}s of 53 and 3.2 μM for A-592107 and A-769662, respectively (Figure 2B). A-769662 also inhibited fatty acid synthesis in mouse hepatocytes (IC_{50} = 3.6 μM, data not shown). These results indicate that both compounds show cellular potencies comparable to those seen in the enzymatic assays using partially purified AMPK. In order to provide a more global comparison of results from the two assays, we performed a Spotfire correlation analysis of data from approximately 170 compounds. As shown in Figure 2C, the EC_{50}s and IC_{50}s generated from enzymatic and cellular assays of the structurally related thienopyridones demonstrated a good correlation

Table 1. Nucleotide levels following 4 hr treatment of primary rat hepatocytes with A-769662

A-769662 Concentration	AMP (nmol/10^6 cells)	ADP (nmol/10^6 cells)	ATP (nmol/10^6 cells)	AMP:ATP
Untreated	0.35	0.78	6.21	0.057
1 μM	0.25	0.89	6.63	0.037
10 μM	0.4	0.93	6.34	0.063
100 μM	0.35	0.95	7.48	0.047

Values given are individual determinations that are representative of three independent experiments.

between the enzymatic potencies and the inhibition of fatty acid synthesis (R = 0.596).

To eliminate the possibility that the inhibition of fatty acid synthesis could be mediated in part by cytotoxicity, we assessed the potential cellular cytotoxicity of the compound series using a colorimetric MTS assay. This assay measures the bioreduction of a tetrazolium salt into a formazan product by dehydrogenase enzymes in metabolically active cells. Treatment of rat hepatocytes with A-769662 at concentrations up to 100 μM showed no measurable cytotoxicity, whereas effects of a known cytotoxic agent, staurosporine, were significant (Figure 2D). Although we demonstrated that A-769662 directly activates AMPK in vitro we wanted to further probe the mechanism of action by assessing whether this compound alters the cellular levels of AMP, ADP or ATP. As shown in Table 1, A-769662 treatment at concentrations up to 100 μM caused no significant alterations in ATP and AMP levels in primary rat hepatocytes. Taken together, these results indicate the thienopyridone AMPK activators exert their cellular effects by direct activation of AMPK activity and not as a consequence of cellular stress, toxicity, or by altering the AMP/ATP ratio.

Acute treatment of SD rats with A-769662

Since AMPK activation inhibits ACC activity, one expected in vivo consequence is a decrease in malonyl CoA levels, leading to reduced lipogenesis and increased fatty acid oxidation. To evaluate this hypothesis we studied the effects of A-769662 on whole-body fatty acid oxidation by indirect calorimetry. Sprague Dawley (SD) rats that were fed ad libitum prior to the study were first acclimated by placing them in a gas exchange indirect calorimeter without food for 2 hr. The animals were then gavaged with a mixed meal [Glucerna (12 ml/kg) plus raw cornstarch (0.5 g/ml)], along with administration of either 30 mg/kg A-769662 (i.p.), 500 mg/kg metformin (oral) or vehicle (i.p.), and monitored for oxygen consumption and CO_2 production for the remaining 14 hr. Vehicle-treated rats preferentially oxidized carbohydrates after the meal bolus as indicated by a respiratory exchange ratio (RER) of close to 1, which is indicative of approximately 100% carbohydrate utilization. In contrast, a single dose of A-769662 or metformin significantly reduced the RER relative to vehicle (RER = 0.81 or 0.86, respectively) throughout the first 3 hr after treatment, indicating increased fatty acid utilization despite the availability of carbohydrates (Figure 3A). This reduction in RER by A-769662 was followed by a small but significant increase in RER versus vehicle over the subsequent 3 hr. The relatively short plasma $t_{1/2}$ of this compound (approximately 3 hr) may explain the transient nature of the single dose effect.

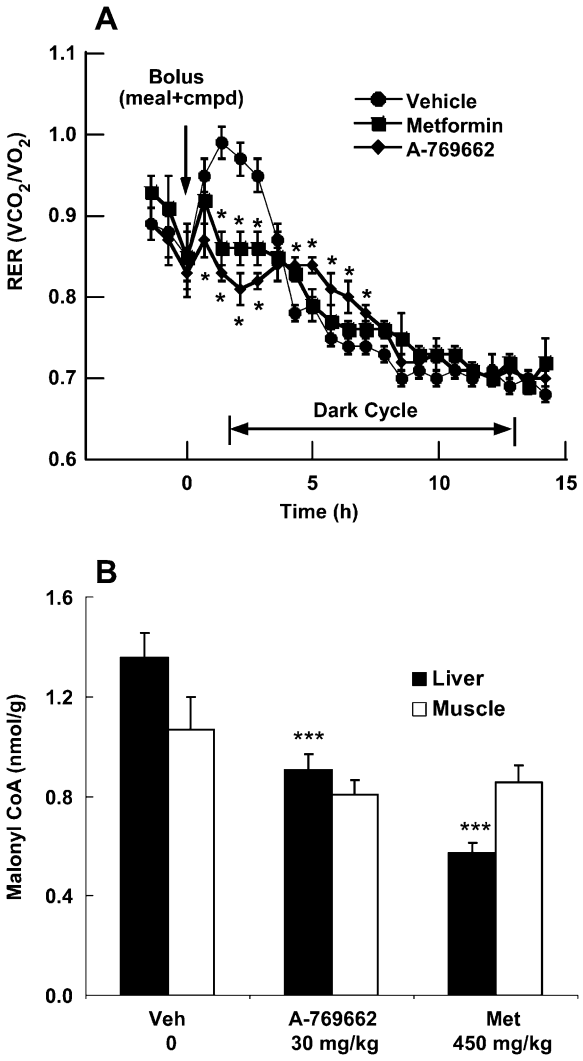

Figure 3. Reduced RER and malonyl CoA levels in SD rats following single treatment with A-769662

Whole-body substrate oxidation, as indicated by the respiratory exchange ratio (RER), and malonyl CoA levels in Sprague Dawley rats treated with a single dose of either vehicle, A-769662 or metformin.

A) SD rats were given a single dose of either vehicle (i.p., n = 12), metformin (p.o., n = 8), or A-769662 (i.p., n = 12) at 4:30 PM (at the initiation of the dark cycle, see Experimental Procedures section) and RER was monitored in an Oxymax chamber for 14 hr. RER values of 0.7 and 1.0 indicate 100% fatty acid and 100% carbohydrate oxidation, respectively. All values are means ± SEM. *, **, ***, $p < 0.05$, < 0.01, < 0.001,versus vehicle, respectively.

B) Malonyl CoA levels were measured in liver and skeletal muscle of SD rats treated as described above. Values are means ± SEM ($n \geq 6$).

In conjunction with increased ACC phosphorylation in primary rat hepatocytes, we anticipated reduced malonyl CoA levels following drug treatment. SD rats were treated with A-769662 or metformin following the same feeding and dosing regimen as described for the indirect calorimetry study above. Liver and muscle tissues were harvested at 1.5 hr postmeal and drug treatment and malonyl CoA levels were measured by LC/MS. We observed 33% and 58% reductions of malonyl CoA levels in livers of animals treated with 30 mg/kg A-769662 (0.905 nmol/g) or 500 mg/kg metformin (0.574 nmol/g), respectively, relative to vehicle controls (1.36 nmol/g, Figure 3B). In addition, we observed a statistically nonsignificant decrease (24% ± 7%,

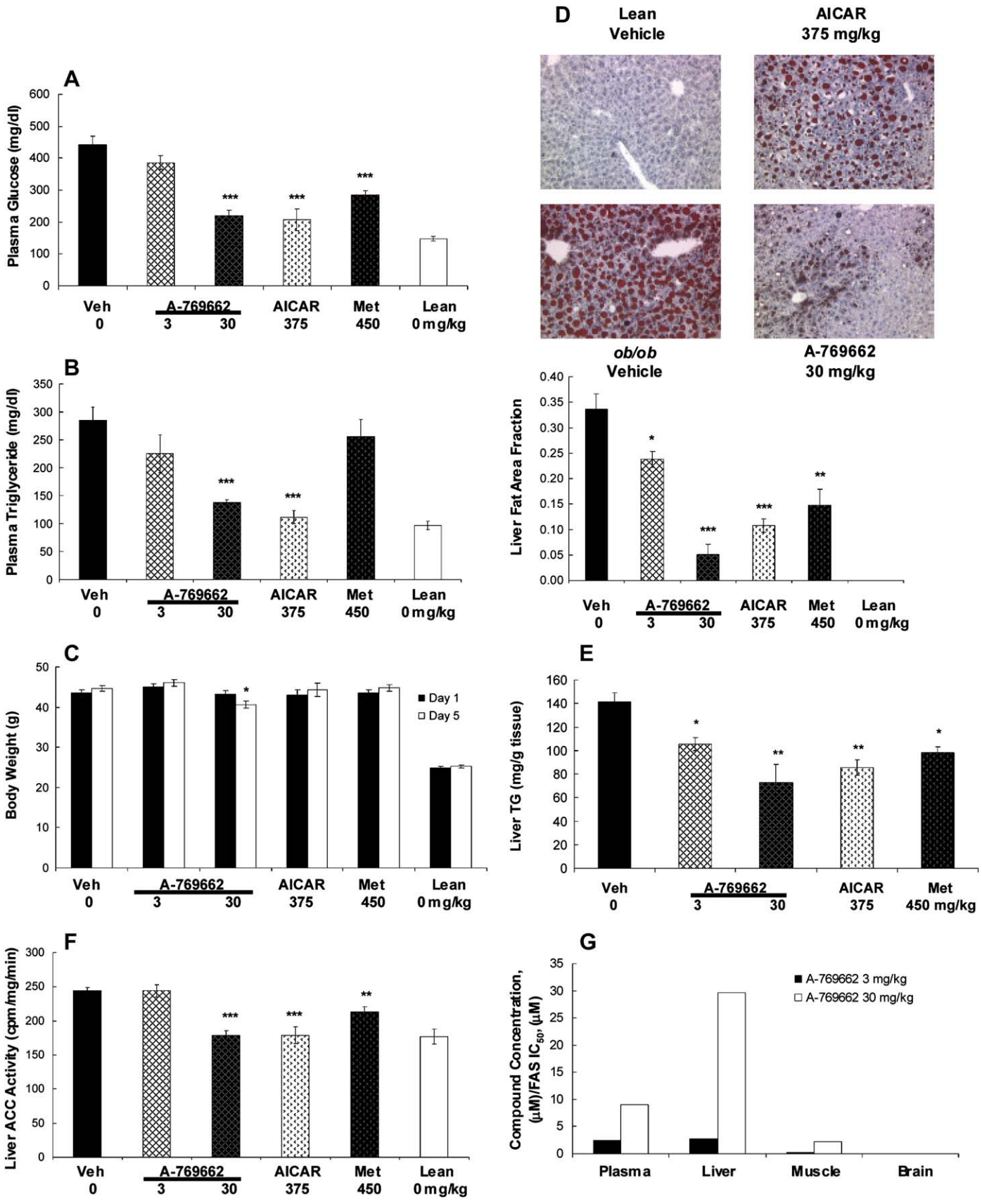
A
Plasma Glucose (mg/dl)
600
500
400
300
200
100
0
***
***
***
Veh
0
A-769662
3
30
AICAR
375
Met
450
Lean
0 mg/kg
B
Plasma Triglyceride (mg/dl)
350
300
250
200
150
100
50
0
***
***
Veh
0
A-769662
3
30
AICAR
375
Met
450
Lean
0 mg/kg
C
Body Weight (g)
50
40
30
20
10
0
*
Day 1
Day 5
Veh
0
A-769662
3
30
AICAR
375
Met
450
Lean
0 mg/kg
F
Liver ACC Activity (cpm/mg/min)
300
250
200
150
100
50
0
***
***
**
Veh
0
A-769662
3
30
AICAR
375
Met
450
Lean
0 mg/kg
D
Lean
Vehicle
AICAR
375 mg/kg
ob/ob
Vehicle
A-769662
30 mg/kg
Liver Fat Area Fraction
0.40
0.35
0.30
0.25
0.20
0.15
0.10
0.05
0.00
*
***
***
**
Veh
0
A-769662
3
30
AICAR
375
Met
450
Lean
0 mg/kg
E
Liver TG (mg/g tissue)
160
140
120
100
80
60
40
20
0
*
**
**
*
Veh
0
A-769662
3
30
AICAR
375
Met
450 mg/kg
G
Compound Concentration, (μM)/FAS IC50, (μM)
35
30
25
20
15
10
5
0
A-769662 3 mg/kg
A-769662 30 mg/kg
Plasma
Liver
Muscle
Brain

p = 0.068) in malonyl CoA levels in skeletal muscle of rats treated with A-769662.

Chronic treatment of *ob*/*ob* mice with A-769662

The acute reduction of malonyl CoA levels in SD rats by A-769662 prompted us to further examine the compound in a chronic model. A-769662 was evaluated in diabetic *ob*/*ob* mice during 5 (Figure 4) or 14 day (Figure 5) dosing. Since oral bioavailability was poor (F = 7%), animals were dosed twice daily by i.p. injection. Metformin (5 and 14 day studies) and AICAR (5 day study) were included as controls. In both studies a 30 mg/kg, b.i.d. dose of A-769662 significantly decreased fed plasma glucose (30%–40% reduction, relative to vehicle), while the lower doses (3 and 10 mg/kg) of A-769662 had no effect (Figures 4A and 5A). On the final day of the studies, the 1 hr postdose glucose level observed with A-769662 (30 mg/kg) was similar to that seen with AICAR (375 mg/kg) or metformin (450 mg/kg). However, the glucose lowering effects of A-769662 (30 mg/kg) in both studies were more sustained than those observed with AICAR or metformin. In the 5 day study, fed glucose levels (16 hr postdose) were lowered by 42%, 7%, or ~2% (compared to vehicle control), following A-769662, AICAR, or metformin treatment, respectively (data not shown). Postprandial insulin levels were not different from vehicle with any of the treatments in the 5 or 14 day studies (data not shown).

In addition to glucose lowering, overall lipid metabolism was modified by A-769662. Plasma samples harvested 1 hr post last dose showed a significant reduction of plasma triglyceride (TG) levels following treatment with A-769662 (30 mg/kg) or AICAR (375 mg/kg) by 54% or 63%, respectively (Figure 4B). There was also a modest reduction in body weight gain in *ob*/*ob* mice treated with 30 mg/kg A-769662 for 5 days (Figure 4C). In the subsequent 14 day study, this initial effect was followed by normal weight gain, similar to that seen in the vehicle control group (Figure 5B). However, at sacrifice in the 14 day study, body weights for the 30 mg/kg A-769662 *ob*/*ob* group remained 9% lower compared to the vehicle control group. Interestingly, this reduction in body weight was accompanied by reductions in liver and epididymal fat pad weights of 27% and 17%, respectively (data not shown), suggesting that lowered fat content most likely accounts for the decreased body weight. Liver TG content decreased dramatically after 5 days of treatment with both doses of A-769662, AICAR, or metformin as assessed by Oil Red O lipid staining (Figure 4D). In addition, by direct measurement of liver triglyceride levels, we observed a statistically significant and dose-responsive lowering by 26% or 48% (relative to vehicle controls) in animals treated with 3 mg/kg or 30 mg/kg A-769662, respectively (Figure 4E). Liver TGs were also lowered significantly (39% and 30%, respectively) in AICAR and metformin treated animals. A decrease in liver TGs was previously observed subsequent to AICAR treatment in fed *ob*/*ob* mice (Song et al., 2002), in high-fat fed rats (Iglesias et al., 2002) and in ZDF rats. However, in contrast with our results and with the results mentioned above, it should be noted that AICAR treatment has been shown to increase liver weight by unknown mechanisms in nonobese rats (Winder et al., 2000) and in obese Zucker (*fa*/*fa*) rats, with an accompanying loss of intraabdominal fat (Buhl et al., 2002). In a more recent short-term study, delivery of adenovirus encoding constitutively active AMPKα2 targeted specifically to liver increased hepatic lipid

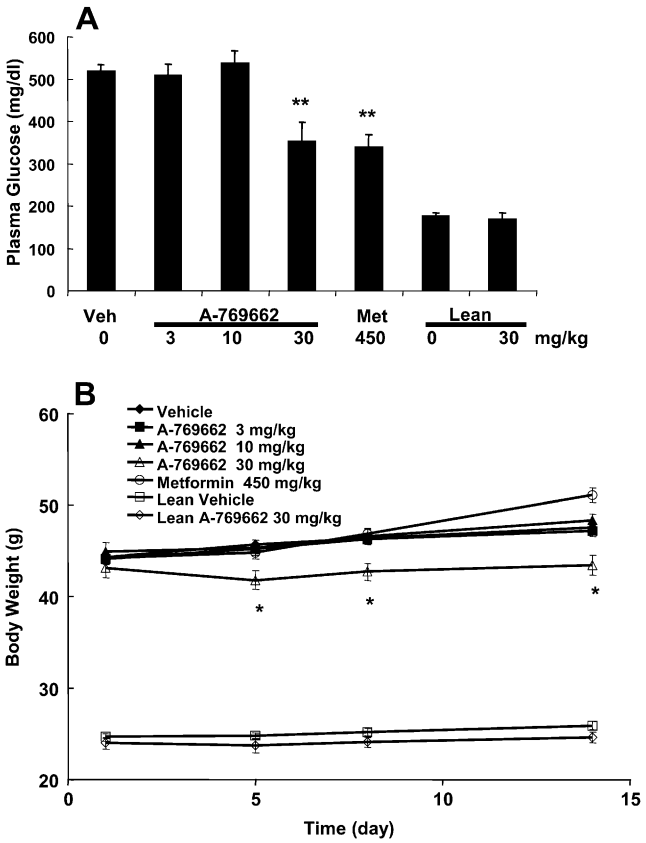

Figure 5. *ob*/*ob* 14 day study showing reduced plasma glucose

Treatment groups were: *ob*/*ob* vehicle or A-769662 (3, 10, or 30 mg/kg, i.p., b.i.d.) or lean littermates treated with vehicle or A-769662 (30 mg/kg) (n = 10 per group).
A) Postprandial plasma glucose levels measured 1 hr post final dose.
B) Body weights at study initiation and over the course of the study.
All values are means ± SEM. p values as described in Figure 3.

Figure 4. Reduced plasma glucose levels, lipids, and ACC activity in 5 day *ob*/*ob* study

6- to 7-week-old *ob*/*ob* and lean littermate mice were studied at baseline and after 5 days treatment (at 8 AM, see Experimental Procedures section). Treatment groups were as follows: *ob*/*ob* mice treated with vehicle (0.2% hydroxypropyl methylcellulose [HPMC], i.p., b.i.d.), A-769662 (3 or 30 mg/kg, i.p., b.i.d.), AICAR (375 mg/kg, s.c., b.i.d.), or metformin (450 mg/kg, p.o., q.d.), and lean littermates treated with vehicle (i.p., b.i.d.), (n = 10 per group).
A) Postprandial plasma glucose levels were measured 1 hr post final dose on day 5.
B) Plasma triglyceride levels on day 5 (1 hr post final dose).
C) Body weights were taken at study initiation and on day 5.
D) Liver fat area fraction was determined by Oil Red O staining at sacrifice (4–5 livers per group were sectioned, stained, and analyzed using MetaMorph image analysis software).
E) In another identical 5 day *ob*/*ob* study, triglyceride levels were determined in livers from fed animals using the Infinity Triglyceride Reagent (n $\geq$ 4).
F) ACC activity in liver was measured after sacrifice and tissue harvest (n = 6).
G) Distribution of A-592107 and A-769662 in tissues harvested 1 hr after final dose (n = 10, except for brain n = 5) is represented as the compound level in tissue divided by its IC_{50} in the fatty acid synthesis cellular assay.
All values are means ± SEM. p values as described in Figure 3.

deposition, as measured by Oil Red O staining (Foretz et al., 2005). Clearly, in our study we did not observe increased hepatic lipid accumulation with A-769662 or AICAR treatment. These results point to a need for further study to clarify the overall consequences of altering lipid and glucose metabolism via AMPK activation, and to the likelihood of animal model and dosing paradigm-dependent variations in findings. We also monitored food consumption in the 14 day study and observed a modest, transient reduction in food intake with A-769662 at 30 mg/kg (5.5 versus 4.5 g/24 hr/mouse) compared to vehicle control. However, no changes in food consumption or body weight (Figure 5B) were observed in lean control mice treated with A-769662 at 30 mg/kg. Additionally, core body temperatures, ALT and AST levels remained unchanged with any of the treatments (data not shown).

To prove that the altered liver fat content observed following A-769662 treatment is mechanism based through AMPK activation, we measured ACC activity in tissues derived from a 5 day *ob/ob* study (Figure 4F). Liver from animals treated with 30 mg/kg A-769662 showed a reduction in ACC activity (179 cpm/mg/min) relative to vehicle control (244 cpm/mg/min). A significant reduction in ACC activity was also noted with 375 mg/kg AICAR (179 cpm/mg/min) and 500 mg/kg metformin (213 mg/kg/min). While we focused on the role of ACC in altering liver fat content, AMPK has also been strongly implicated in the regulation of sn-glycerol-3-phosphate acyltransferase (G3PAT) activity (Muoio et al., 1999). Since G3PAT catalyzes the committed step in glycerolipid biosynthesis thus playing a regulatory role in the partitioning of acyl-CoA toward β-oxidation, the potential exists for A-769662 to be exerting it's influence on lipid metabolism through multiple mechanisms in addition to modulation of ACC activity.

HPLC analysis of tissue drug exposures revealed that A-769662 reached the highest concentration in liver, with much lower levels in muscle, and almost undetectable levels in brain (Figure 4G). We used compound concentrations required for the inhibition of fatty acid synthesis in isolated hepatocytes as a comparator for compound levels observed to elicit pharmacodynamic effects. Compound concentrations observed in liver 1 hr after administration of 30 mg/kg or 3 mg/kg of A-769662 were approximately 30-fold or 2.5-fold, respectively, above the cellular IC_{50} for fatty acid synthesis. In muscle, the cellular IC_{50} was exceeded by 2.2-fold after 30 mg/kg A-769662, but was not reached at 3 mg/kg. It is tempting to speculate that a higher exposure in skeletal muscle would lead to a more sustained increase in overall whole-body fatty acid oxidation and energy expenditure.

Since glucose lowering following A-769662 treatment was observed in both the 5 and 14 day study, we evaluated the potential mechanism leading to this result by quantitating gluconeogenic gene expression. Previous studies showed a decrease in PEPCK and/or glucose-6-phosphatase (G6Pase) expression in vitro subsequent to AICAR or metformin treatment (Lochhead et al., 2000; Morioka et al., 2005) In vivo, suppression of gluconeogenic gene expression in conjunction with AMPK activation was reported in mouse liver following injection of full-length adiponectin (Yamauchi et al., 2002) or during short-term overexpression of constitutively active AMPK via adenovirus-mediated gene transfer (Foretz et al., 2005; Viana et al., 2006). To explore the possible mechanism responsible for glucose lowering with A-769662, we evaluated PEPCK, G6Pase, and FAS (fatty acid synthase) gene expression in liver following an acute (24 hr) or chronic (5 day) treatment using real-time quantitative RT PCR analysis (Figure 6A). For both treatment durations, animals were fasted overnight prior to sacrifice, and the livers were harvested 1 hr post final dose.

In the acute treatment (Figure 6A), A-769662 had no significant effects on PEPCK, G6Pase or FAS. In contrast, PEPCK gene expression was modestly but significantly decreased with AICAR (19%). To our surprise, however, there was a dramatic increase in G6Pase mRNA expression (435%), as well as a modest induction of FAS mRNA (62%) by AICAR. Metformin did not significantly regulate PEPCK or G6Pase but FAS gene expression was lowered by 35%. We extended these findings by evaluating hepatic gene expression following 5 days of treatment (Figure 6A), where we observed a significant decrease in PEPCK (37%), G6Pase (63%), and FAS (31%) mRNA expression with A-769662. In contrast, AICAR decreased PEPCK expression (30%) and, similar to the acute study, increased G6Pase (325%) and FAS (100%) mRNA expression. We did not detect significant changes in gene expression following 5 day metformin treatment. Based on these findings we believe that A-769662 most likely mediates its metabolic actions in part via hepatic AMPK activation leading to modulation of gluconeogenic gene expression.

Because the effect of AICAR on G6Pase and FAS expression was entirely unexpected, we evaluated PEPCK, G6Pase, and FAS expression in liver samples from fed or fasted *ob/ob* and lean mice under the identical PCR conditions used above. As anticipated, we observed decreased PEPCK and G6Pase and increased FAS expression in fed compared to fasted animals (Figure 6B), thus validating the QPCR methodology used for the gene expression analysis. Although AICAR has been shown to decrease PEPCK and G6Pase expression in vitro, (Lochhead et al., 2000) comparable in vivo experiments have not been reported. We speculate that AMPK-independent inhibition of FBPase by AICAR (via ZMP) with resulting inhibition of gluconeogenesis induces compensatory changes, including increased G6Pase, to maintain hepatic glucose output. We currently have no explanation for the unexpected increase in FAS mRNA observed after AICAR treatment, but assume that it is not AMPK-mediated since it was not observed with metformin or A-769662 treatment.

In contrast to AICAR, prolonged treatment with A-769662 not only lowers PEPCK mRNA levels but, as anticipated, it also decreases G6Pase and FAS expression. These results are in good agreement with previously published results demonstrating decreased PEPCK and G6Pase expression in *ob/ob* and streptozotocin-induced diabetic mice following adenovirus-mediated transfer of constitutively active AMPK (Foretz et al., 2005). Similarly, the reduction in FAS expression subsequent to A-769662 treatment recapitulates results obtained in experiments in normal, fasted/refed mice following adenovirus-mediated overexpression of AMPK (Foretz et al., 2005) and in SD rats subsequent to metformin treatment (Zhou et al., 2001).

Under fasting conditions, we demonstrated a decrease in gluconeogenic gene expression with A-769662 but did not observe a significant decrease in glucose levels (data not shown). We speculate that this discrepancy may be due to the timing of gene regulation, the duration of fasting period, or the much smaller difference in glucose levels observed between the *ob/ob* vehicle and the lean control mice with overnight fasting. However, the robust glucose lowering observed under fed conditions accompanied by the decrease in PEPCK and G6Pase

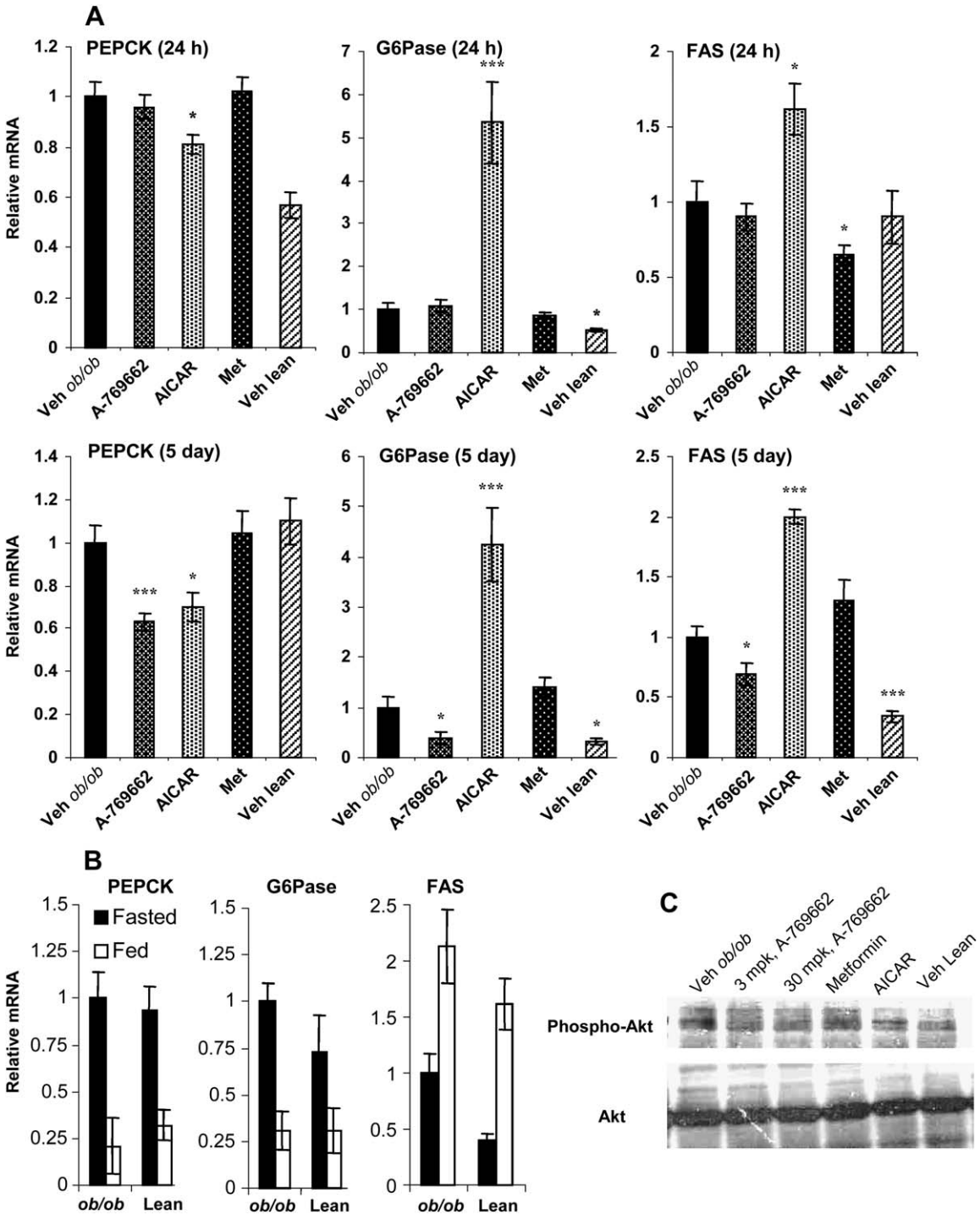

Figure 6. Reduced gluconeogenic gene expression and lack of Akt phosphorylation with A-769662

6- to 7-week-old *ob/ob* and lean littermate mice were studied after 24 hr or 5 days treatment (at 8 AM, see Experimental Procedures section and Figure 4 legend). Animals were dosed as previously described but fasted overnight and the tissues harvested 1 hr post last dose.

A) Real-time quantitative RT PCR analysis was used to measure PEPCK, G6Pase, and FAS mRNA levels in RNA samples from livers of fasted animals. PCR was performed in duplex including primers to 28S RNA for normalization. The 5 day results shown are representative of two independent animal experiments ($n \geq 9$).

B) Real-time quantitative mRNA analysis was done using liver RNA samples from fed (a subset of mice, n = 5 per group, were fed overnight prior to dosing and sacrifice) and fasted animals and PEPCK, G6Pase, and FAS mRNAs measured. As above, all samples were run in duplex with 28S RNA ($n \geq 4$).

All values given are means ± SEM. p values as given in Figure 3.

C) Total Akt or phospho-Akt levels in protein lysates from livers of fed animals as detected by Western analysis.

expression in A-769662 treated animals strongly suggests that the decreased expression of gluconeogenic genes contributes to the modulation of glucose levels by A-769662.

As in our previous 14 day study, estimated food intake was monitored in a 5 day study. In agreement with the 14 day study, we observed a transient decrease in estimated food intake in the

30 mg/kg A-769662 dose group (~42% at day 3, $p < 0.05$ versus vehicle) but this level was similar to that observed for AICAR and metformin. As mentioned in the Experimental Procedures section, the *ob*/*ob* mice were group-housed, 5 animals/cage, therefore we can only provide a crude estimate of individual food intake. In the 14 day study, glucose lowering was accompanied by food intake and body weight normalization to near vehicle control levels, suggesting that decreased food intake most likely is not the primary mechanism for glucose and lipid lowering. Furthermore, in the 5 day study, food intake was measured on day 3, while treatment efficacy was determined on day 5 when food intake was increasing. However, we cannot completely rule out the possibility that the transient reduction in food intake influenced the observed endpoint efficacy including changes in gene expression.

Weight loss might be expected with prolonged peripheral tissue stimulation of the AMPK pathway and the resultant inactivation of ACC. Increased lipid oxidation and energy expenditure combined with resistance to high fat diet-induced weight gain was observed in ACC2 knockout mice (Abu-Elheiga et al., 2003). In addition, AMPK KO mice subjected to a high-fat diet exhibit increased body weight and fat mass, relative to wild-type controls (Villena et al., 2004). The results described above illustrate the significance of AMPK activation and ACC2 regulation in sustaining energy homeostasis and in regulating whole-body metabolism. Conversely, recent reports describe increased food intake in animals i.c.v. injected with AICAR (Andersson et al., 2004; Kim et al., 2004), indicating a divergence in the effects of peripheral versus central AMPK activation. The lack of increased food intake in A-769662-treated animals could be due to the absence of compound exposure in the brain.

We also questioned whether the effects of A-769662 could be due to action through an alternate, AMPK-independent, secondary pathway. We examined Akt phosphorylation and found no changes in phosphorylated (active) Akt levels in livers from 5 day A-769662-treated animals (Figure 6C), arguing against secondary effects of A-769662 via the Akt pathway.

Taken together, our results indicate that specific, small molecule-mediated activation of AMPK improves overall glucose and lipid metabolism. Based on the tissue distribution of our compounds, it is likely that the effects observed in mice are primarily due to stimulation of AMPK in liver. The decrease in plasma and liver TG levels can be explained by increased oxidation and decreased synthesis of fatty acids in liver. This decrease in hepatic lipid accumulation will subsequently improve insulin-sensitivity, resulting in improved glucose metabolism. Although compound exposure in skeletal muscle of mice treated with 30 mg/kg A-769662 was modest, we cannot exclude the possibility that AMPK activation in skeletal muscle contributes to the whole-body efficacy observed with A-769662. However, there is literature precedence demonstrating the impact of liver targeted AMPK activation. A recent study of short-term, liver specific, overexpression of a constitutively active form of AMPKα2 in obese and diabetic mouse models highlights many of the expected benefits of AMPK activation (Foretz et al., 2005). Liver selective AMPK overexpression led to decreased blood glucose levels and gluconeogenic gene expression in normal, streptozotocin-induced and *ob*/*ob* diabetic mice and to decreased circulating lipid levels and increased hepatic fatty acid oxidation in normal C57BL/6j mice (Foretz et al., 2005). Thus, the liver specific AMPK activation was sufficient to induce a switch from glucose to fatty acid utilization to supply energy needs.

Many of the studies validating AMPK stimulation as a potential target for the treatment of type 2 diabetes, obesity and the metabolic syndrome have utilized AICAR as a tool to induce AMPK activation. Since AICAR is metabolized to ZMP, an AMP mimetic, it clearly has additional effects that are independent of AMPK activation. In both rat hepatocytes (Vincent et al., 1991) and in mice in vivo (Vincent et al., 1996) AICAR was shown to dose-dependently inhibit fructose-1,6-bisphosphatase activity hence potently inhibiting gluconeogenesis. More recently, metformin and TZDs have been shown to activate AMPK, however, both of these agents are indirect and nonselective. While AMPK activation is an attractive approach for the regulation of lipid and glucose metabolism, studies utilizing direct and selective AMPK activators as with the current study are needed to clearly isolate and elucidate the myriad effects of AMPK activation.

Overall, our results demonstrate that small molecule-mediated direct stimulation of AMPK in vivo is feasible. Our data also strengthen the hypothesis that AMPK activation primarily directed to liver can affect whole-body intermediary metabolism with improvements in circulating levels of glucose and lipids. This further supports the potential of AMPK as a drug target for the treatment of diabetes and the metabolic syndrome.

Experimental procedures

Preparation of enzyme

Following a previously described modification (Anderson et al., 2004) of an established protocol (Hawley et al., 1996), partially purified AMPK was prepared from rat livers, hearts or skeletal muscles (Pel Freez, Rogers, Arizona). To purify AMPK from HEK293 cells, frozen cell pellets were homogenized in the previously described Buffer A containing EDTA-free protease inhibitor (Roche Diagnostics GMBH) and Benzonase (EM Industries, Hawthorne, New York). The homogenate was centrifuged 30 min at 10,000 × g and the supernate decanted, brought to 1% PEG (average 8000 MW) and mixed for 30 min. Following clarification of the sample by centrifugation the purification proceeded as previously described and the active fractions were pooled and concentrated using an Amicon stirred cell concentrator (Millipore).

The AMPK isoform, $\alpha 1\beta 1\gamma 1$, was cloned and expressed in a baculovirus/Sf9 system. Sf9 cells were grown in Sf900 II SFM media (Gibco, Carlsbad, California) to a cell density of 2.5×10^6 cells/ml in Wave Bioreactors (Wave Biotech, Bridgewater New Jersey), at which point the culture was infected with three separate baculovirus stocks encoding the α, β, and γ chains. Each virus was added to a multiplicity of infection (MOI) of 2.0. Cells were harvested 48 hr postinfection by centrifugation and the resulting paste stored at −85°C until processing following a modification of the protocols described above.

All steps described above were carried out at 4°C and all chemicals were supplied by Sigma unless otherwise noted.

96-well AMPK assay

AMPK activity was measured by monitoring phosphorylation of the SAMS peptide substrate (20 μM in standard assays and 100 μM in additivity assays) following a previously described protocol (Anderson et al., 2004). To determine whether compound-induced AMPK activation occurs in a reversible manner, AMP or A-769662 were preincubated with rat liver AMPK for 10 min at 20 times standard assay concentrations prior to dilution and measurement of AMPK activity. Unless otherwise specified, chemicals used in the above assay were supplied by Sigma.

Glycogen phosphorylase b assay

To assay glycogen phosphorylase b (GPb) activity (Kaiser et al., 2001), 1.5 μg/ml of rabbit GPb was added to a reaction mix containing 20 mM Na_2HPO_4 (pH 7.2), 2 mM $MgSO_4$, 1 mM β-NADP (β-nicotinamide adenine dinucleotide phosphate), 1.4 U/ml G-6-PDH (Glucose-6-Phosphate-Dehydrogenase) and

3 U/ml PGM (phosphoglucomutase). AMP or test compounds were added to the assay medium at the specified concentrations followed by the addition of glycogen (final concentration 1 mg/ml) to initiate the reaction. After incubating 10 min at 25ºC, GPb activity was assessed by measuring absorbance at 340 nm. All reagents for the GPb assay were from Sigma.

Fructose 1,6-bis-phosphatase assay

D-fructose-1,6 diphosphatase (FBPase, 0.01 U/ml final concentration) in 2× assay buffer, 100 mM Tris (pH 7), 4 mM $MgCl_2$, 300 mM NaCl, 0.2 mg/ml BSA and 6 mM DTT, was added to test compounds to give final concentrations as indicated. Substrate, D-fructose-1,6-diphosphate, at a final concentration of 0.1 mM was added to the reaction and the reaction mix was incubated at 30ºC for 20 min. Following the incubation 2 volumes of Malachite Green solution (Upstate, Charlottesville, Virginia) containing 0.001% Tween 20 was added and absorbance at 640 nm read immediately. Unless otherwise stated, reagents used for this assay were supplied by Sigma.

ACC and Akt phosphorylation

For ACC studies, hepatocytes were isolated from 8 week old, male, Sprague Dawley rats by collagenase (Sigma) digestion (Ulrich et al., 1995; Van den Berghe et al., 1980). and plated at 1×10^6 cells per well in collagen coated 6-well plates (Becton Dickinson Labware). Following an overnight serum starvation cells were treated for 4 hr with test compounds at the concentrations described and lysed in RIPA buffer (PBS [Gibco], 1% NP40 [Sigma], 0.5% SDC, [Sigma], 0.1% SDS [Sigma], and Protease Inhibitor Cocktail [Sigma]). For Akt studies, livers were homogenized using a Tissumizer (Tekmar Co., Cincinnati, Ohio) in a 1:10 volume (w/v) of RIPA buffer, homogenates were centrifuged at 15,000 × g for 60 min at 2ºC, and the upper lipid layer removed by aspiration. Following electrophoresis and transblotting, total ACC levels were measured using NeutrAvidin alkaline phosphatase (Pierce, Rockford, Illinois) and the alkaline phosphatase substrate, Immunopure FastRed (Pierce). The primary, polyclonal antibodies used were specific for phospho-ACC (Upstate, Lake Placid, New York), phospho-Akt (Cell Signaling Technology, Beverly, Massachusetts) or Akt (Cell Signaling Technology). In each case an HRP-conjugated secondary antibody (Amersham, Buckinghamshire, England) was used and Westerns were developed in ECL (Amersham).

Fatty acid synthesis assay

The protocol described below is an adaptation of methods previously described (Foretz et al., 1998; Garcia-Villafranca et al., 2003). Primary rat hepatocytes were isolated as described above and plated at 5×10^4 cells per well on BioCoat, collagen-coated, black-walled 96-well plates (Becton Dickinson Labware, Bedford, Massachusetts) in DMEM (Gibco) supplemented with 10% FBS (Hyclone, Logan, Utah), 5 mM glucose (Sigma), 1 mM sodium pyruvate (Gibco), 2 mM L-glutamine (Gibco), 25 mM HEPES (Gibco), 0.1 mM nonessential amino acids (Gibco), 5 μg/ml transferrin (Gibco), 100 nM dexamethasone (Sigma), 100 nM insulin (Sigma) and 25 μg/ml gentamycin (Gibco). After 4 hr medium was replaced with medium as described above but without FBS and containing 100 nM triiodothyronine (T_3) (Sigma). Following a 16 hr, 37ºC incubation, the incubation medium was removed and replaced with medium containing ^{14}C acetate (2 μCi/ml, Perkin Elmer) and AICAR (Sigma) or test compounds at the indicated concentrations. Cells were incubated 4 hr at 37ºC then the plates were rinsed with PBS (Gibco). The final wash was replaced with Microscint20 (Perkin Elmer) and radioactivity incorporated into fatty acid monitored on a Wallac (Turku, Finland) Microbeta plate reader.

Compound potencies in enzymatic and cellular assays were correlated by Spotfire Decision Site™ analysis (Spotfire, Inc. Somerville, Massachusetts).

Cytotoxicity assay

Primary rat hepatocytes were isolated and treated as described for the fatty acid synthesis assay. Following a 4 hr treatment with test compounds, medium was removed from the cells and replaced with medium containing MTS reagent (Promega, Madison,Wisconsin). Plates were incubated at 37ºC to allow for color development and cell viability was evaluated by conversion of a tetrazolium salt into a formazon product measured spectrophotometrically at 490 nm.

AMP:ATP assay

Primary rat hepatocytes were plated and treated as described for the determination of ACC phosporylation. Following the 4 hr incubation with compound, cells were washed with ice-cold PBS (Gibco) and the adenine nucleotides were extracted as previously described (Corton et al., 1994) with 500 μl/well $HClO_3$. The acid was extracted with three treatments of 1.1 volumes of 1:1 tri-n-octylamine:1,1,2-trichlorotriflouroethane and 50-100 μl of the aqueous sample injected on a Whatman (Brockville, Ontario, Canada) Partisil 10 SAX column preequilibrated in Buffer A (10 mM K_2PO_4, [pH 6.75]). To elute, sample columns were run for 5 min in Buffer A, then for 15 min in a linear gradient to Buffer B (500 mM K_2HPO_4, [pH 5]) and finally for 35 min in Buffer B at a flow rate of 2 ml/min. To measure nucleotide concentration absorbance was read at 254 nm. Unless otherwise indicated, all reagents were supplied by Sigma.

Animal care and treatment

ob/ob mice and their lean littermates (6–7 weeks of age, Jackson Laboratories, Bar Harbor, Maine) and Sprague Dawley (SD) rats of 200-220 g (Charles River, St. Louis, Missouri) were acclimated to the animal research facilities for 5 days. The following investigations were conducted in accordance with Abbott Laboratories IACUC guidelines. *ob/ob* mice were housed 5 per cage, and lean *ob*/+ littermates 2 per cage, and maintained on mouse chow (Labdiets #5015, St. Louis, Missouri) ad libitum. The SD rats were single housed and were further acclimated to an indirect calorimeter gas exchange system (Oxymax, Columbus Instruments, Columbus, Ohio), overnight on two occasions prior to study.

Gas exchange in Sprague Dawley rats

After acclimation to the indirect calorimetery system the SD rats were taken off their normal rat chow (Labdiets #5002, Richmond, Indiana) and given a high-sucrose diet (Research Diets AIN-76A, 70% sucrose, New Brunswick, New Jersey) as reported previously (Harwood et al., 2003). They were placed in the indirect calorimeter at 2:30 PM, denied access to food, and 2 hr later given an oral meal challenge, raw cornstarch (0.5 g/ml, ARGO, CPC International, Englewood Cliffs, New Jersey) in a mixed liquid meal of Glucerna (12 ml/kg, Abbott Laboratories, Columbus, Ohio), by gavage, immediately followed by either vehicle (0.2% HPMC, i.p. n = 12), metformin (500 mg/kg, p.o., n = 8), or A-769662 (30 mg/kg, i.p., n = 12). This mixed bolus of nutrients provides a low but sustained glucose response and was provided at the start of their normal dark cycle. VO_2, VCO_2 and respiratory exchange ratio (RER, VCO_2/VO_2) were monitored.

Malonyl CoA assay

Malonyl CoA levels were measured in SD rat tissues from animals treated with the same feeding paradigm as described above and sacrificed 1.5 hr after drug treatment. Tissues were harvested, immediately frozen in liquid nitrogen and then homogenized in a 1:10 volume (w/v) of ice-cold 5% sulfosalicylic acid containing 50 μM dithioerythritol. Homogenates were centrifuged at 15,000 × g for 60 min at 2ºC and the supernatants filtered through a 0.22 micron filter (Ultrafree-MC, Millipore Corporation, Bedford, Massachusetts). Samples were stored at –80ºC prior to liquid chromatography mass spectrometry analysis. HPLC was run at binary mode (A: 5 mM dimethylbutylamine and 6 mM HOAc; B: 0.1% formic acid in CH_3CN [EMD Chemicals, Gibbstown, New Jersey]) at 200 μL/min with the third pump to deliver post column mixing solvent CH_3CN. The data were acquired on an Applied Biosystem Pulsar I quadrapole-TOF mass spectrometer (Foster City, California) using positive ion TOFMS mode (Lan Gao, 2005 ASMS conference abstract). Reagents were supplied by Sigma unless stated otherwise.

***ob/ob* studies**

After acclimation *ob/ob* and lean mice were randomized to the various treatment groups by body weight and fed glucose levels (tail snip) at 8 AM. Baseline plasma insulin samples were also taken from a subset of the animals representing each treatment group (n = 10 *ob/ob* and n = 10 lean *ob*/+ littermates; ELISA, ALPCO Diagnostics, Windham, NH). Two separate *ob/ob* and lean littermate studies were completed: 1) an initial 5 day study, and 2) a 14 day study to examine efficacy and more completely characterize the body weight change observed in the 5 day study. Treatment groups for the 5 day study were as follows: *ob/ob* vehicle (0.2% hydroxypropyl methylcellulose [HPMC], i.p., b.i.d.), A-592107 (10 or 100 mg/kg, i.p., b.i.d.),

A-769662 (3 or 30 mg/kg, i.p., b.i.d.), AICAR (375 mg/kg, s.c., b.i.d.), or metformin (450 mg/kg, p.o., q.d., with vehicle in PM), and lean littermates treated with vehicle (i.p., b.i.d.), (n = 10 per group). Treatment groups for the 14 day *ob/ob* and lean littermate study were as follows: *ob/ob* vehicle (0.2% HPMC, i.p., b.i.d.), A-769662 (3, 10, or 30 mg/kg, i.p., b.i.d.), or metformin (as described above for the 5 day study) (n = 10 per group), and lean littermates treated with vehicle or 30 mg/kg of A-769662 (i.p., b.i.d.).

For the 5 day study plasma glucose levels were determined at baseline as described above, and 1 hr post dose on day 5 at 9 AM. After animals were weighed and blood samples were taken, animals were sacrificed by CO_2 asphyxiation followed by a cardiac venipuncture. In the 14 day study nonfasting plasma glucose levels (tail snip) were determined at baseline on day 1 (as described above), and days 5, 8, and 14 and 1 hr postdose for these days. After measurements were taken, animals were sacrificed as described above. For both experiments terminal blood samples were used for determination of plasma insulin, FFA and triglyceride levels. Additionally, the following tissues were harvested and frozen immediately in liquid nitrogen for further analysis: liver, epididymal fat pad, skeletal muscle, and brain.

Two additional *ob/ob* experiments were performed under the same conditions as described above. In the first, mice (n = 10 per group) were sacrificed after an overnight fast and either 24 hr or 5 days of dosing. Following randomization mice were dosed *bid,* fasted overnight prior to sacrifice, and dosed 1 hr prior to sacrifice. In the second, both overnight fasted (n = 10 per group) and postprandial (n = 5 per group) sacrifice conditions on day 5 at 9 AM (1 hr postfinal dose) were studied. Estimated food intake was determined in this study for the first 3 days of the experiment by food weight difference from days 0-to-1, 1-to-2 and 2-to-3. There were n = 15 mice per treatment arm and they were housed 5 per cage, therefore data are from each of the 3 cages for each treatment divided by the number of mice/cage, mean±S.E.

Processing and analysis of samples from *ob/ob* experiments

Plasma glucose was determined in tail snip samples by the glucose oxidase method (Precision PCx glucose meter, Abbott Laboratories, North Chicago, Illinois). Day 5 1 hr post dose plasma insulin samples were taken from each treatment group (ELISA, ALPCO Diagnostics, Windham, New Hampshire). Plasma free fatty acids (FFAs) and triglycerides (TGs) were determined by standard enzymatic assays (FFA, Wako, Richmond, Virginia and TG, Sigma, St. Louis, Missouri, respectively). Liver fat area fraction in tissue sections was determined by Oil Red O (Poly Scientific, Bay Shore, New York) staining. Images were acquired using a Leica DMIRE microscope (Leica Microsystems, Wetzlar, Germany), an Optronics DEI-750 video camera (Optronics, Goleta, California) and MetaMorph software (Universal Imaging, Downington, Pennsylvania). Ten random images were taken from each tissue section, using a 20× microscope objective and a motorized scanning stage. Images were analyzed using MetaMorph image analysis software. The images were thresholded to detect the Oil Red O stained fat droplets. Plasma and tissue levels of A-592107 and A-769662 were determined by HPLC.

ACC activity assay

ACC activity was assayed by measuring the incorporation of $(^{14}C)HCO_3^-$ into malonyl CoA. Tissues were homogenized in a 10× volume (w/v) of buffer containing 50 mM Tris (pH 7.4), 2 mM DTT, 2.5 mg/ml sucrose, 0.6 mg/ml digitonin and Protease Inhibitor Cocktail and homogenates were centrifuged at 15,000 × g for 100 min at 2ºC. After normalizing protein concentrations ACC activity was measured in 96-well, white-walled plates (Wallac) using an assay reaction mix of 50 mM Hepes (pH 7.5) 10 mM potassium citrate, 10 mM $MgCl_2$, 4 mM potassium carbonate (pH 8.3), 0.5 mM ATP, 0.4 mM $NaH^{14}CO_3$ (Perkin Elmer), 0.25 mM acetyl CoA and 0.075% fatty acid-free BSA. Plates were incubated at RT for 40 min before stopping the reaction with the addition of .5 volume of 1 N HCl and allowed to stand ON at RT to release unincorporated ^{14}C. Scintillant was added (OptiPhase SuperMix, Perkin Elmer) and cpm measured using a Wallac Micro-Beta counter. Unless otherwise noted, all reagents were supplied by Sigma.

Quantitation of mRNA

Total RNAs were extracted from liver using the Qiazol method (Qiagen, Valencia, California). and the mRNA quantitated using a Platinum qRT-PCR kit (Invitrogen) and an Applied Biosystems thermocycler. Primers were as follows for 28S RNA, 28ST (Hex-TCA-CGACGGTCTAAACCCAGCTCACG), 28SF (TGTCTGAACCTGCGGTTCCCT), 28SR (TTCACCAAGCGTTCGATTGTT) (Integrated DNA Technologies, Coralville, Iowa). Primers used for PEPCK were PEPCK(T) (FAM-TGGCCAGCGCATGCGG), PEPCKF (GAAGGACAGACTCGCCCTATGT, PEPCKR (CAGGGGCCTCCAGC-ACAGAT) (Integrated DNA Technologies). Primers for G6Pase were G6Pase(T) (Fam-TGCTCCCATTCCGTTCGCC, G6PaseF (TGCAAGGGAGAACTGAGCAA), G6PaseR (GGACCAAGGAAGCCACAATG) (Qiagen). Primers used for FAS were FAS(T) (Fam-CACCAGAGATGCTCCGATCCCCA), FASF (TCCCCAGTTCCTGCACTCA), FASR (TCCCCAGTTCCGCACTCA) (Operon Technologies, Alameda, California). All samples were run in duplex with and normalized to 28S RNA.

Liver triglycerides

Liver tissue was homogenized in thirty volumes of ethanol (Polytron homogenizer, Brinkmann, Westbury, New York). Samples were vortexed, allowed to settle and the supernatant was centrifuged at 15,000g for 10 min at room temperature. To assay, 10 μl of PBS was first added to flat bottom polystyrene plates (Nalge Nunc, Westchester, New York) followed by 2.5 μl of cleared supernatant. 300 μl Infinity Triglyceride Reagent (Thermo Electron, Melbourne, Australia) was added to wells and the plate was incubated at 37ºC for 5 min. After cooling to room temperature, samples were read at 520 nm with a SpectraMax Plus spectrophotometer (Molecular Devices, Sunnyvale, California).

Cross-reactivity assays

Cross-reactivity assays were performed by CEREP (www.cerep.com).

Supplemental data

Supplemental data include one table and can be found with this article online at http://www.cellmetabolism.org/cgi/content/full/3/6/403/DC1/.

Acknowledgments

We thank Christine Collins, Rebecca Gum, Amanda Mika, Martin Voorbach, Hua Tang, Lan Gao, Xueheng Cheng, Richard Janis, Larry Solomon, Karl Walter, Marc Lake, Steven Postl, David Egan, Paul Richardson, and Leo Barrett for advice and experimental support. All authors are or were formerly employees of Abbott Laboratories.

Received: July 29, 2005
Revised: December 1, 2005
Accepted: May 17, 2006
Published: June 6, 2006

References

Abu-Elheiga, L., Oh, W., Kordari, P., and Wakil, S.J. (2003). Acetyl-CoA carboxylase 2 mutant mice are protected against obesity and diabetes induced by high-fat/high-carbohydrate diets. Proc. Natl. Acad. Sci. USA *100*, 10207–10212.

Anderson, S.N., Cool, B.L., Kifle, L., Chiou, W., Egan, D.A., Barrett, L.W., Richardson, P.L., Frevert, E.U., Warrior, U., Kofron, J.L., and Burns, D.J. (2004). Microarrayed compound screening (microARCS) to identify activators and inhibitors of AMP-activated protein kinase. J. Biomol. Screen. *9*, 112–121.

Andersson, U., Filipsson, K., Abbott, C.R., Woods, A., Smith, K., Bloom, S.R., Carling, D., and Small, C.J. (2004). AMP-activated protein kinase plays a role in the control of food intake. J. Biol. Chem. *279*, 12005–12008.

Buhl, E.S., Jessen, N., Pold, R., Ledet, T., Flyvbjerg, A., Pedersen, S.B., Pedersen, O., Schmitz, O., and Lund, S. (2002). Long-term AICAR administration reduces metabolic disturbances and lowers blood pressure in rats displaying features of the insulin resistance syndrome. Diabetes *51*, 2199–2206.

Carling, D. (2004). The AMP-activated protein kinase cascade–a unifying system for energy control. Trends Biochem. Sci. *29*, 18–24.

Carling, D., Zammit, V.A., and Hardie, D.G. (1987). A common bicyclic protein kinase cascade inactivates the regulatory enzymes of fatty acid and cholesterol biosynthesis. FEBS Lett. *223*, 217–222.

Corton, J.M., Gillespie, J.G., and Hardie, D.G. (1994). Role of the AMP-activated protein kinase in the cellular stress response. Curr. Biol. *4*, 315–324.

Davies, S.P., Carling, D., and Hardie, D.G. (1989). Tissue distribution of the AMP-activated protein kinase, and lack of activation by cyclic-AMP-dependent protein kinase, studied using a specific and sensitive peptide assay. Eur. J. Biochem. *186*, 123–128.

Davies, S.P., Sim, A.T., and Hardie, D.G. (1990). Location and function of three sites phosphorylated on rat acetyl-CoA carboxylase by the AMP-activated protein kinase. Eur. J. Biochem. *187*, 183–190.

Foretz, M., Ancellin, N., Andreelli, F., Saintillan, Y., Grondin, P., Kahn, A., Thorens, B., Vaulont, S., and Viollet, B. (2005). Short-term overexpression of a constitutively active form of AMP-activated protein kinase in the liver leads to mild hypoglycemia and fatty liver. Diabetes *54*, 1331–1339.

Foretz, M., Carling, D., Guichard, C., Ferre, P., and Foufelle, F. (1998). AMP-activated protein kinase inhibits the glucose-activated expression of fatty acid synthase gene in rat hepatocytes. J. Biol. Chem. *273*, 14767–14771.

Fryer, L.G., Parbu-Patel, A., and Carling, D. (2002). The Anti-diabetic drugs rosiglitazone and metformin stimulate AMP-activated protein kinase through distinct signaling pathways. J. Biol. Chem. *277*, 25226–25232.

Garcia-Villafranca, J., Guillen, A., and Castro, J. (2003). Involvement of nitric oxide/cyclic GMP signaling pathway in the regulation of fatty acid metabolism in rat hepatocytes. Biochem. Pharmacol. *65*, 807–812.

Goldstein, B.J., and Scalia, R. (2004). Adiponectin: A novel adipokine linking adipocytes and vascular function. J. Clin. Endocrinol. Metab. *89*, 2563–2568.

Hardie, D.G. (2003). Minireview: the AMP-activated protein kinase cascade: the key sensor of cellular energy status. Endocrinology *144*, 5179–5183.

Hardie, D.G., and Hawley, S.A. (2001). AMP-activated protein kinase: the energy charge hypothesis revisited. Bioessays *23*, 1112–1119.

Hardie, D.G., Scott, J.W., Pan, D.A., and Hudson, E.R. (2003). Management of cellular energy by the AMP-activated protein kinase system. FEBS Lett. *546*, 113–120.

Harwood, H.J., Jr., Petras, S.F., Shelly, L.D., Zaccaro, L.M., Perry, D.A., Makowski, M.R., Hargrove, D.M., Martin, K.A., Tracey, W.R., Chapman, J.G., et al. (2003). Isozyme-nonselective N-substituted bipiperidylcarboxamide acetyl-CoA carboxylase inhibitors reduce tissue malonyl-CoA concentrations, inhibit fatty acid synthesis, and increase fatty acid oxidation in cultured cells and in experimental animals. J. Biol. Chem. *278*, 37099–37111.

Hawley, S.A., Boudeau, J., Reid, J.L., Mustard, K.J., Udd, L., Makela, T.P., Alessi, D.R., and Hardie, D.G. (2003). Complexes between the LKB1 tumor suppressor, STRADalpha/beta and MO25alpha/beta are upstream kinases in the AMP-activated protein kinase cascade. J. Biol. *2*, 28.

Hawley, S.A., Davison, M., Woods, A., Davies, S.P., Beri, R.K., Carling, D., and Hardie, D.G. (1996). Characterization of the AMP-activated protein kinase kinase from rat liver and identification of threonine 172 as the major site at which it phosphorylates AMP-activated protein kinase. J. Biol. Chem. *271*, 27879–27887.

Iglesias, M.A., Ye, J.M., Frangioudakis, G., Saha, A.K., Tomas, E., Ruderman, N.B., Cooney, G.J., and Kraegen, E.W. (2002). AICAR administration causes an apparent enhancement of muscle and liver insulin action in insulin-resistant high-fat-fed rats. Diabetes *51*, 2886–2894.

Kahn, B.B., Alquier, T., Carling, D., and Hardie, D.G. (2005). AMP-activated protein kinase: ancient energy gauge provides clues to modern understanding of metabolism. Cell Metab. *1*, 15–25.

Kaiser, A., Nishi, K., Gorin, F.A., Walsh, D.A., Bradbury, E.M., and Schnier, J.B. (2001). The cyclin-dependent kinase (CDK) inhibitor flavopiridol inhibits glycogen phosphorylase. Arch. Biochem. Biophys. *386*, 179–187.

Kemp, B.E., Mitchelhill, K.I., Stapleton, D., Michell, B.J., Chen, Z.P., and Witters, L.A. (1999). Dealing with energy demand: the AMP-activated protein kinase. Trends Biochem. Sci. *24*, 22–25.

Kim, E.K., Miller, I., Aja, S., Landree, L.E., Pinn, M., McFadden, J., Kuhajda, F.P., Moran, T.H., and Ronnett, G.V. (2004). C75, a fatty acid synthase inhibitor, reduces food intake via hypothalamic AMP-activated protein kinase. J. Biol. Chem. *279*, 19970–19976.

Lochhead, P.A., Salt, I.P., Walker, K.S., Hardie, D.G., and Sutherland, C. (2000). 5-aminoimidazole-4-carboxamide riboside mimics the effects of insulin on the expression of the 2 key gluconeogenic genes PEPCK and glucose-6-phosphatase. Diabetes *49*, 896–903.

Longnus, S.L., Wambolt, R.B., Parsons, H.L., Brownsey, R.W., and Allard, M.F. (2003). 5-Aminoimidazole-4-carboxamide 1-beta-D-ribofuranoside (AICAR) stimulates myocardial glycogenolysis by allosteric mechanisms. Am. J. Physiol. Regul. Integr. Comp. Physiol. *284*, R936–R944.

McGarry, J.D., and Brown, N.F. (1997). The mitochondrial carnitine palmitoyltransferase system. From concept to molecular analysis. Eur. J. Biochem. *244*, 1–14.

Minokoshi, Y., and Kahn, B.B. (2003). Role of AMP-activated protein kinase in leptin-induced fatty acid oxidation in muscle. Biochem. Soc. Trans. *31*, 196–201.

Minokoshi, Y., Kim, Y.B., Peroni, O.D., Fryer, L.G., Muller, C., Carling, D., and Kahn, B.B. (2002). Leptin stimulates fatty-acid oxidation by activating AMP-activated protein kinase. Nature *415*, 339–343.

Morioka, K., Nakatani, K., Matsumoto, K., Urakawa, H., Kitagawa, N., Katsuki, A., Hori, Y., Gabazza, E.C., Yano, Y., Nishioka, J., et al. (2005). Metformin-induced suppression of glucose-6-phosphatase expression is independent of insulin signaling in rat hepatoma cells. Int. J. Mol. Med. *15*, 449–452.

Muoio, D.M., Seefeld, K., Witters, L.A., and Coleman, R.A. (1999). AMP-activated kinase reciprocally regulates triacylglycerol synthesis and fatty acid oxidation in liver and muscle: evidence that sn-glycerol-3-phosphate acyltransferase is a novel target. Biochem. J. *338*, 783–791.

Musi, N., Hirshman, M.F., Nygren, J., Svanfeldt, M., Bavenholm, P., Rooyackers, O., Zhou, G., Williamson, J.M., Ljunqvist, O., Efendic, S., et al. (2002). Metformin increases AMP-activated protein kinase activity in skeletal muscle of subjects with type 2 diabetes. Diabetes *51*, 2074–2081.

Ruderman, N., and Prentki, M. (2004). AMP kinase and malonyl-CoA: targets for therapy of the metabolic syndrome. Nat. Rev. Drug Discov. *3*, 340–351.

Ruderman, N.B., Saha, A.K., and Kraegen, E.W. (2003). Minireview: malonyl CoA, AMP-activated protein kinase, and adiposity. Endocrinology *144*, 5166–5171.

Saha, A.K., Avilucea, P.R., Ye, J.M., Assifi, M.M., Kraegen, E.W., and Ruderman, N.B. (2004). Pioglitazone treatment activates AMP-activated protein kinase in rat liver and adipose tissue in vivo. Biochem. Biophys. Res. Commun. *314*, 580–585.

Saha, A.K., Schwarsin, A.J., Roduit, R., Masse, F., Kaushik, V., Tornheim, K., Prentki, M., and Ruderman, N.B. (2000). Activation of malonyl-CoA decarboxylase in rat skeletal muscle by contraction and the AMP-activated protein kinase activator 5-aminoimidazole-4-carboxamide-1-beta -D-ribofuranoside. J. Biol. Chem. *275*, 24279–24283.

Scott, J.W., Hawley, S.A., Green, K.A., Anis, M., Stewart, G., Scullion, G.A., Norman, D.G., and Hardie, D.G. (2004). CBS domains form energy-sensing modules whose binding of adenosine ligands is disrupted by disease mutations. J. Clin. Invest. *113*, 274–284.

Song, X.M., Fiedler, M., Galuska, D., Ryder, J.W., Fernstrom, M., Chibalin, A.V., Wallberg-Henriksson, H., and Zierath, J.R. (2002). 5-Aminoimidazole-4-carboxamide ribonucleoside treatment improves glucose homeostasis in insulin-resistant diabetic (ob/ob) mice. Diabetologia *45*, 56–65.

Steinberg, G.R., Rush, J.W., and Dyck, D.J. (2003). AMPK expression and phosphorylation are increased in rodent muscle after chronic leptin treatment. Am. J. Physiol. Endocrinol. Metab. *284*, E648–E654.

Tomas, E., Tsao, T.S., Saha, A.K., Murrey, H.E., Zhang Cc, C., Itani, S.I., Lodish, H.F., and Ruderman, N.B. (2002). Enhanced muscle fat oxidation and glucose transport by ACRP30 globular domain: acetyl-CoA carboxylase inhibition and AMP-activated protein kinase activation. Proc. Natl. Acad. Sci. USA *99*, 16309–16313.

Ulrich, R.G., Bacon, J.A., Cramer, C.T., Peng, G.W., Petrella, D.K., Stryd, R.P., and Sun, E.L. (1995). Cultured hepatocytes as investigational models for hepatic toxicity: practical applications in drug discovery and development. Toxicol. Lett. *82–83*, 107–115.

Van den Berghe, G., Bontemps, F., and Hers, H.G. (1980). Purine catabolism in isolated rat hepatocytes. Influence of coformycin. Biochem. J. *188*, 913–920.

Viana, A.Y., Sakoda, H., Anai, M., Fujishiro, M., Ono, H., Kushiyama, A., Fukushima, Y., Sato, Y., Oshida, Y., Uchijima, Y., et al. (2006). Role of hepatic AMPK activation in glucose metabolism and dexamethasone-induced regulation of AMPK expression. Diabetes Res. Clin. Pract., in press.

Villena, J.A., Viollet, B., Andreelli, F., Kahn, A., Vaulont, S., and Sul, H.S. (2004). Induced adiposity and adipocyte hypertrophy in mice lacking the AMP-activated protein kinase-alpha2 subunit. Diabetes *53*, 2242–2249.

Vincent, M.F., Erion, M.D., Gruber, H.E., and Van den Berghe, G. (1996). Hypoglycaemic effect of AICAriboside in mice. Diabetologia *39*, 1148–1155.

Vincent, M.F., Marangos, P.J., Gruber, H.E., and Van den Berghe, G. (1991). Inhibition by AICA riboside of gluconeogenesis in isolated rat hepatocytes. Diabetes *40*, 1259–1266.

Viollet, B., Andreelli, F., Jorgensen, S.B., Perrin, C., Geloen, A., Flamez, D., Mu, J., Lenzner, C., Baud, O., Bennoun, M., et al. (2003). The AMP-activated protein kinase alpha2 catalytic subunit controls whole-body insulin sensitivity. J. Clin. Invest. *111*, 91–98.

Winder, W.W., and Hardie, D.G. (1999). AMP-activated protein kinase, a metabolic master switch: possible roles in type 2 diabetes. Am. J. Physiol. *277*, E1–E10.

Winder, W.W., Holmes, B.F., Rubink, D.S., Jensen, E.B., Chen, M., and Holloszy, J.O. (2000). Activation of AMP-activated protein kinase increases mitochondrial enzymes in skeletal muscle. J. Appl. Physiol. *88*, 2219–2226.

Wu, X., Motoshima, H., Mahadev, K., Stalker, T.J., Scalia, R., and Goldstein, B.J. (2003). Involvement of AMP-activated protein kinase in glucose uptake stimulated by the globular domain of adiponectin in primary rat adipocytes. Diabetes *52*, 1355–1363.

Yamauchi, T., Kamon, J., Minokoshi, Y., Ito, Y., Waki, H., Uchida, S., Yamashita, S., Noda, M., Kita, S., Ueki, K., et al. (2002). Adiponectin stimulates glucose utilization and fatty-acid oxidation by activating AMP-activated protein kinase. Nat. Med. *8*, 1288–1295.

Young, M.E., Radda, G.K., and Leighton, B. (1996). Activation of glycogen phosphorylase and glycogenolysis in rat skeletal muscle by AICAR–an activator of AMP-activated protein kinase. FEBS Lett. *382*, 43–47.

Zang, M., Zuccullo, A., Hou, X., Nagata, D., Walsh, K., Herscovitz, H., Brecher, P., Ruderman, N.B., and Cohen, R.A. (2004). AMP-activated protein kinase is required for the lipid-lowering effect of metformin in insulin-resistant human HepG2 cells. J. Biol. Chem. *279*, 47898–47905.

Zhou, G., Myers, R., Li, Y., Chen, Y., Shen, X., Fenyk-Melody, J., Wu, M., Ventre, J., Doebber, T., Fujii, N., et al. (2001). Role of AMP-activated protein kinase in mechanism of metformin action. J. Clin. Invest. *108*, 1167–1174.

Zou, M.H., Kirkpatrick, S.S., Davis, B.J., Nelson, J.S., Wiles, I.W., Schlettner, U., Neumann, D., Brownlee, M., Freeman, M.B., and Goldman, M.H. (2004). Activation of the AMP-activated protein kinase by the anti-diabetic drug metformin in vivo: Role of mitochondrial reactive nitrogen species. J. Biol. Chem. *279*, 43940–43951.